

Chapter 11

Double Purpose Drilling Fluid Based on Nanotechnology: Drilling-Induced Formation Damage Reduction and Improvement in Mud Filtrate Quality



Johanna V. Clavijo, Leidy J. Roldán, Diego A. Castellanos, German A. Cotes, Ángela M. Forero, Camilo A. Franco, Juan D. Guzmán, Sergio H. Lopera, and Farid B. Cortés

11.1 Introduction

The production in the Ocelote field is mainly in C7 sand, which corresponds to sand from the Carbonera formation. The well logs recorded during the life cycle of this field show drilling-induced formation damage associated with the drilling process where water-based drilling fluids have been used. Therefore, the production from the new wells was low based on the values estimated from the petrophysical properties. Although this problem has been alleviated by modifying the type and design of the bridging material used in the conventional fluids, there is scope to further reduce the damage and achieve an early stimulation of the formation from other types of mechanisms. Moreover, during the production life of the wells, the productivity decreases because of fines migration (presence of migratory clays) and wettability changes due to organic deposits (crude oil with colloidal instability).

J. V. Clavijo · S. H. Lopera

Grupo de Investigación en Yacimientos de Hidrocarburos, Facultad de Minas, Universidad Nacional de Colombia – Sede Medellín, Medellín, Colombia
e-mail: jovargascl@unal.edu.co; shlopera@unal.edu.co

L. J. Roldán · C. A. Franco (✉) · J. D. Guzmán · F. B. Cortés (✉)

Química Grupo de Investigación en Fenómenos de Superficie—Michael Polanyi, Departamento de Procesos y Energía, Facultad de Minas, Universidad Nacional de Colombia, Sede Medellín, Medellín, Colombia
e-mail: lejroldanya@unal.edu.co; caafancoar@unal.edu.co; dguzmanc@unal.edu.co; fbcortes@unal.edu.co

D. A. Castellanos · G. A. Cotes · Á. M. Forero

Hocol S.A., Bogotá, Colombia
e-mail: diego.castellanos@hocol.com.co; german.cotes@hocol.com.co; Angela.forero@hocol.com.co

Mud filtrate and solid particle invasion near the wellbore during the drilling process and the consequent formation damage induced are the main problems in the oil and gas industry [1–3]. The different damage mechanisms due to the mud filtrate are associated with polymer adsorption onto the rock and plugging [1], ionic incompatibility between the filtrate and the formation water [4], aqueous filtrate trapping [5], wettability [6, 7], and pore-blocking effects [8] resulting from changes in the saturation of water [9, 10]. The solid and fine particles inherent to the formation block the pore throats and reduce the effective flow space [11, 12]. Furthermore, an accurate interpretation of the well logs depends strongly on the depth of the mud filtrate and fine mobilization extent.

It is difficult to reduce the near-wellbore invasion of the mud filtrate and mitigate the fines migration given the design of the drilling fluids in terms of the selection of suitably sized bridging material [13–16] and filtration control additives [17] for an appropriate filter cake development [18]. Moreover, the properties of the reservoir and formation fluids, particularly the viscosity, interfacial tension (IFT), and wettability, vary because of the interactions between the reservoir fluid, mud filtrate, and fine particles [10]. Therefore, in the drilling fluid design, reducing the drilling-induced formation damage due to the invasion of the mud filtrate and controlling the fines migration are essential. The solution designed in this study aims to mitigate the formation damage while drilling a well in a field located in the Llanos Basin of Colombia (Ocelote field).

Recently, nanoparticles (NPs) have been employed in NP-based drilling fluids, where the NPs influence the viscosity, filtration control, and thermal and electrical conductivities, among the other properties of the drilling fluid simultaneously [19]. For instance, authors have evaluated the chemical characteristics of NPs [20–23], intercalated clay hybrid [24, 25], and nano-polymer material [26–28] to improve the rheological behavior and filtration properties of the drilling fluids. Others have studied carbon nanotubes, SiO₂, ZnO, and CuO NPs to enhance the thermal and electrical conductivities [19, 29–31]. Some studies have demonstrated that NPs could improve shale inhibition and wellbore stability [32–34]. However, these studies did not consider the inhibition of the formation damage due to the drilling fluids. Moreover, these NP-based drilling fluids neglect the effects of the mud filtrate and fine invasion into the porous media. Most studies focused on bentonite-based drilling fluids, which are associated with a high formation damage degree [35, 36].

More recently, our research group examined the effects of the nanoparticle size and surface acidity on the formation damage due to bentonite-free water-based drilling fluids. Additionally, the authors found that the invaded mud filtrate remained in contact with the heavy oil during the displacement and reduced the viscosity [37]. Therefore, nanofluids should be designed such that they not only reduce the formation damage but also ensure that the mud filtrate invaded allows inhibiting the damage mechanism such as in terms of the fine migration, wettability alteration, and viscosity reduction, while additionally acting as a drilling fluid for stimulation treatment. The NPs could favor the stimulation of the reservoir and reduce the use of additional chemical stimulation treatments for improving the oil and gas production in the early stages. Recently, Al-Yasiri et al. [19] developed a multifunctional

drilling fluid by incorporating NPs. This nanofluid improved the rheology, filtration, and thermal properties of the drilling fluid, overcoming many of the difficulties encountered in drilling operations [19]. To the best of our knowledge, there is no report that addresses both the reduction in drilling-induced formation damage and enhancement in the mud filtrate quality that could improve the oil mobility and help control fines migration with the use of a mud filtrate invaded with NPs.

Therefore, in this study, we designed a double purpose nanofluid to reduce the drilling-induced formation damage while the mud filtrate invaded allows for improving the oil mobility and controlling the migration fines through core flooding tests under reservoir conditions. Our double purpose drilling fluid is a new concept for NP-based drilling fluids to reduce the drilling-induced formation damage while improving the quality of the mud filtrate invaded, allowing for the interaction between the rock and the formation fluids. Improvement in oil mobility and better fines migration control can be expected. This paper is organized into five main sections: (i) NP characterization, (ii) evaluation of rheological and filtration properties, (iii) evaluation of the mud filtrate quality, (iv) core flooding experiments, and (v) field application. Our experimental study on the drilling fluids could help enhance the drilling fluid properties, reduce the drilling-induced formation damage, and employ the mud filtrate as an early stimulation treatment to improve the oil mobility by reducing the wettability change and IFT. Field applications were carried out on the drilling of two horizontal wells, in which a high mud filtration invasion has been historically reported. The results are validated by comparing the behavior of the pilot with a base drilling fluid well whose drilling is carried out using the same drilling fluid but without the nanomaterials. The wells are evaluated in terms of the invasion diameter, well stabilization time, productivity index, and solid production, in order to verify the effectiveness of the NPs in the drilling fluid.

11.2 Materials and Methods

11.2.1 Nanoparticle Characterization

Fumed silica NPs (Si, 99%, Sigma Aldrich, United States) and β -alumina NPs (Al, Petroraza, Colombia) were used. The NPs were characterized using the hydrodynamic diameter ($d_h = 9.7 \pm 4$ nm Si and 61.4 ± 6 nm Al) and zeta potential at pH of work (ζ -potential @ pH 10 = -31.54 ± 3 mV Si and -56.66 ± 2 mV Al) based on the dynamic light scattering technique (DLS) using a Nanoplus-3 from Micrometrics (Norcross, GA, United States). The surface area (SBET = 380 m²/g Si and 247 m²/g Al) was determined through N₂ physisorption using the Brunauer–Emmett–Teller method (BET) with a Gemini VII 2390 Surface Area Analyzer (Autosorb-1 from, Quantachrome, United State). Finally, the Fourier transform infrared spectroscopy (FTIR) using an IRAffinity-1 s (Shimadzu, Kyoto, Japan) was applied to determine the functional groups on the NP surface.

11.2.2 Drilling Fluid Preparation and Characterization

The drilling fluid was prepared to blend each component in a mixer (Hamilton Beach, United State) as follows: 300 mL of water, pH was adjusted with caustic soda to reach a value of 10 (NaOH >98%, Sigma Aldrich, United State), 1 g of xanthan gum (Sigma Aldrich, United State), 5 g of starch (Sigma Aldrich, United State), 22 g of diesel, 3.4 g of 600 mesh calcium carbonate (CaCO₃, Procomin, Colombia), 15.0 g of 325 mesh CaCO₃, and 4.1 g of 200 mesh CaCO₃. The Al and Si NPs were added after xanthan gum with a concentration varying from 0 to 0.3 wt.%.

11.2.3 Methods

11.2.3.1 Aging Process

Each of the prepared drilling fluid samples was aged in a hot roller oven (Fann, United States) in a hermetic cylinder at 76 °C for 16 h by adhering to the American Petroleum Institute (API) recommended test procedures [38]. The objective was to evaluate the rheology and filtration control in the worst scenario of the drilling fluid, that is, after thermal and dynamic degradation during the drilling operation under the bottom hole conditions.

11.2.3.2 Rheological and Filtration Test

A rotational viscometer (Ofite, United States) was used to determine the rheological properties of the drilling fluid. The plastic viscosity (PV) was obtained by subtracting the Fann values at θ_{600} and θ_{300} . Yield point (YP) was obtained by subtracting at the PV value the Fann lecture at θ_{300} . Gel strength was measured at 10 s and 10 min (Gel 10s/10 m) reading the maximum dial at θ_3 after at the respective time of not circulation. Finally, the HPHT filtration test (Fann, United States) was conducted to quantify the filtration volume under the static condition with a differential pressure of 500 psi and a temperature of 76 °C, respectively. Additionally, the mudcake thickness was measured using a digital caliper (700–113 MyCal Lite, Mitutoyo America Corp, United State) with several repetitions. These procedures adhered to the standard protocols of the API [38].

Based on the results of the rheological and filtration experiments, the optimal concentration of the NPs was selected to evaluate the performance of the mud filtrate obtained in their respective filtration test for improving the oil mobility and fines migration control.

11.2.3.3 Contact Angle, Spontaneous Imbibition Test, and Interfacial Tension Measurements

The oil-wet rock samples, representative of the formation mineralogy, were immersed into the mud filtrates with and without the NPs for 24 h at 25 °C. The rock samples were oil-wet induced by asphaltene precipitation from an intermediate heavy crude (23° API and asphaltene content of 10.54% by weight) produced from the Ocelote field. Subsequently, the contact angle was measured through the sessile drop method using an Attention Theta optical tensiometer (Biolin Scientific, Finland). Moreover, we conducted a spontaneous test on the imbibition of water into the oil-wet rock impregnated previously with the mud filtrate, before drying at 70 °C overnight, at room temperature to monitor the weight changes in the system after being submerged. The imbibed water mass was recorded for 3.5 h [39, 40]. The wettability changes were analyzed on the basis of the liquid/air/rock contact angles formed in the surface samples treated with the filtrate mud with and without the NPs and in the differences between the imbibed mass. Finally, the IFT between the crude oil/water formation and the crude oil/mud filtrate with and without the NPs was evaluated at 25 °C using a force tensiometer - K11 (Krüss, Germany). The same crude oil used for the oil-wet induction was employed for the IFT measurements and the displacement test.

11.2.3.4 Fines Retention Experimental Test

Fines retention experimental tests were performed in synthetic porous media previously impregnated with the mud filtrate with and without the NPs under atmospheric conditions. The porous media were prepared with 70 g of Ottawa sand (Minercol S.A, Colombia) (12–20 and 25–40 mesh) in a fraction mass of 50% ratio of each mesh. The solution of the fines was composed of a mass fraction of 0.2% kaolinite, because it is considered the most problematic clay and the main reason for the plugging of porous spaces due to its migration [41–43], as seen in the Ocelote field. Hence, fines suspension was injected from the top and flowed through the sand packed through gravity forces. The effluent was collected and passed through the filter paper to measure the quantity or concentration of the fines retained. Before the test, the sand bed was soaked for 24 h with the mud filtrate with the NPs to impregnate the porous media. The filter paper was weighted each time the fines suspension passed through the porous media, thus determining the fines retained using an analytical balance (A & D company, United States) and obtaining the concentration of the resultant fines. The test was completed once the initial concentration was equal to the effluent concentration [42, 44].

11.2.3.5 Displacement Test

Sandstone core samples from the Carbonera C7 formation of the Ocelote field were used to compare the formation damage by the solid particle and mud filtrate invasion from the drilling fluids with and without the NPs and to evaluate the migratory clay control through the invaded mud filtrate. The mineralogical composition of the rock samples consists of quartz (86%), feldspar (2%), illite/smectic (1%), illite/mica (1%), kaolinite (9%), and chlorite (1%). The core flooding experiments were carried out under reservoir and dynamic conditions such as a reservoir pressure of 1627 psi, a confining pressure of 2293 psi, an injection rate of 0.3 mL/min, and a temperature of 76 °C. Table 11.1 lists the basic properties of the core samples from the Ocelote field.

The drilling-induced formation damage due to the drilling fluid was evaluated by comparing the permeability values before and after the injection of the drilling fluid with respect to the protocol by Van der Zwaag [45]. The NP performance was examined considering three scenarios: (1) baseline, (2) drilling fluid injection without NPs, and (3) drilling fluid with NPs, in other words the double purpose drilling fluid. First, a synthetic brine was injected, and the absolute permeability was measured (Kabs). Subsequently, the Ko and relative permeability curves (Kr) were obtained through the injection of the crude oil and synthetic brine, respectively. The crude oil was injected to reach the residual water saturation state. Thereafter, the drilling fluid was circulated in the transverse direction to the production core face with an overbalance pressure of 500 psi, simulating the drilling operative times and appropriate rates of the field. Additionally, while drilling with fluid circulation, the dynamic filtration was measured. Later, the oil effective permeability (Ko) was evaluated by injecting the crude oil. The Kro, Krw, and oil recovery factors after the drilling mud circulation were measured during the injection of the synthetic brine until the residual oil saturation (Sor). Finally, the crude oil was injected, and the return permeability was measured.

To evaluate the fines migration control by the mud filtrate invaded into the core, the drilling fluid with and without the NPs was once again circulated over the core face. The experimental protocol to determine the critical injection rate was based on a study conducted by Cespedes et al. [42]. Crude oil was injected at injection rates of 0.1, 0.3, 0.5, 1.0, 2.0, 3.0, 5.0, and 7.0 mL/min to obtain the injection rate in which Ko is reduced by 10% compared with the previous Ko value.

Table 11.1 Permeability and porosity core samples of the core samples from Carbonera C7 formation of Ocelote field

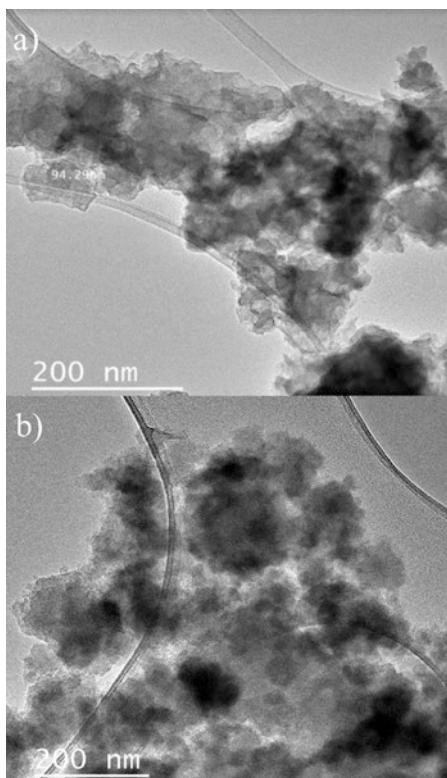
Core number	Permeability (mD)	Pore volume (mL)	Porosity (%)
1	453	9.7	20.2
2	445	11.1	22.0

11.3 Results

11.3.1 Nanoparticle Characterization

Figure 11.1 shows the transmission electron microscopy (TEM) images. The NPs presented an irregular form, and it was possible to corroborate the nanometric size obtained by the DLS. Figure 11.2 presents the FTIR spectrum and vibrational absorption bands for the Al and Si NPs. The representative bands of the vibration of the silica (Si–OH, Si–O–Si), alumina (Al–OH, Al–O–Al), and hydroxyl (–OH) groups can be observed. The wide peak in the range of $3000\text{--}3550\text{ cm}^{-1}$ is associated with Al–OH and Si–OH bonds and adsorbed water molecules on the surface in the case of both the NPs [46]. The peak at approximately 808 cm^{-1} can be attributed to siloxane (Si–O–Si) symmetric vibrations. The peak in the range of $980\text{--}1220\text{ cm}^{-1}$ corresponds to Al–O–Al and Si–O–Si linkages. Additionally, the band Si–O–Si groups are responsible for the peak in the range of $1970\text{--}1840\text{ cm}^{-1}$ [47]. The FTIR of the NPs is similar, except for the dissimilarities in the intensity of the peaks for the –OH groups. The surface area of the Si NPs is larger than that of the Al NPs, so

Fig. 11.1 Transmission electron microscopy images (TEM) of (a) Al and (b) Si NPs at a magnification of 200 nm



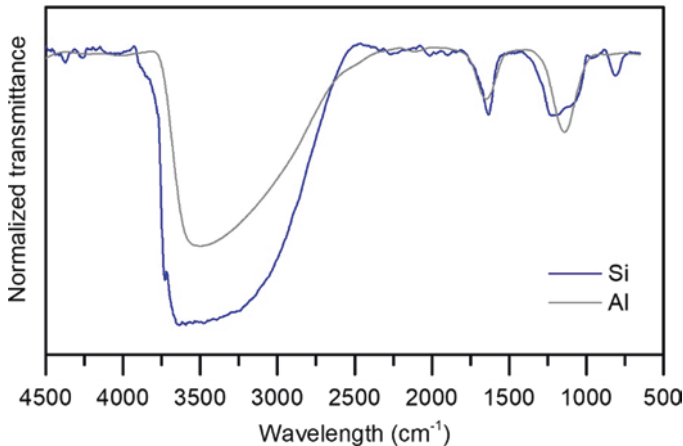


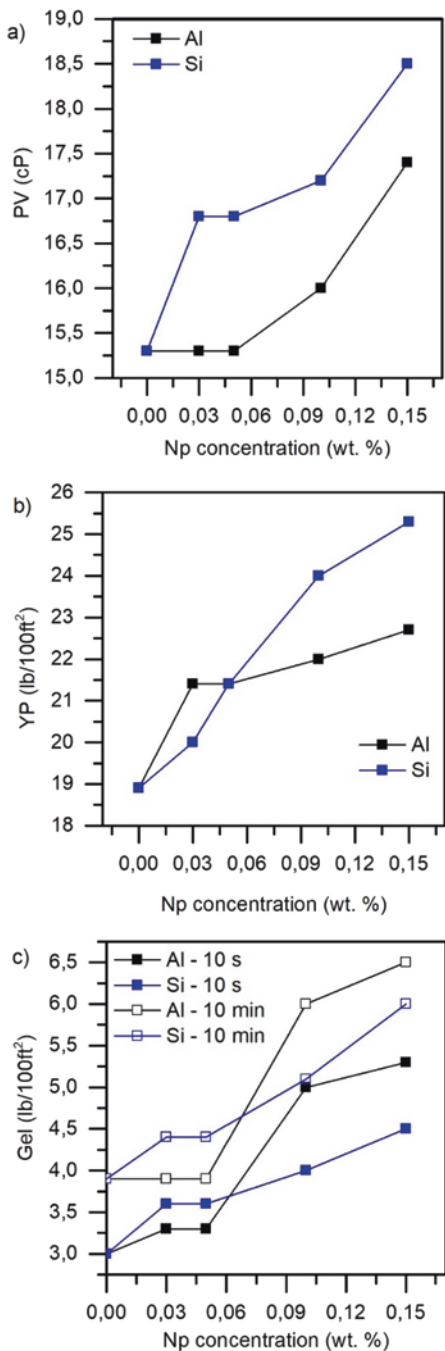
Fig. 11.2 FTIR spectra of Al and Si nanoparticles

the presence of $-OH$ groups could be more representative; even water is adsorbed onto the surface in the case of the Si NPs.

11.3.2 Rheological and Filtration Behaviors

Figure 11.3a–c show the NP concentration effect on the PV, YP, and gel strength at 70 °C, respectively, of the drilling fluid samples after the hot rolling process, representing the critical scenario of the drilling fluids during the operation due to the thermal degradation. As expected, the PV increases with the increase in the NP concentration in the system. However, for Al NP concentrations in the range of 0.03–0.05 wt.%, the PV did not increase. In fact, at a concentration of 0.1 wt.% and higher, the PV increased. The Si NPs presented a higher PV increment than Al NPs. This increment in the PV values is a result of the adsorption of the hydrophilic group of the NPs with the polymer through hydrogen bonding with the $-OH$ groups on the NP surface [48, 49]. However, the Si NPs had a stronger interaction with the polymer. The Al NPs had a lower adsorption capacity than silica [50]. The high PV can be attributed to the viscous base fluid; it means that there is an alteration of the cross-linking effect [51]. The addition of solid particles and the increment in the viscosity did not represent changes in the density of the drilling fluids, conserving the value of 8.9 lb/gal in all the samples. The addition of solid particles did not change the hydrostatic pressure of the fluid, thus ensuring a safe drilling operation. The YP presents a similar behavior as the PV values. The YP values increase with the increase in the NP concentration. However, the effect was stronger in the case of YP than in the case of PV after the addition of the NPs. The average increments for the PV were 5% and 13% for the Al and Si NPs, respectively, whereas for the YP, the increments were 16% and 20%. The YP is considered the flow resistance as a

Fig. 11.3 Rheological properties of the drilling fluid samples as a function of the NP concentration: (a) plastic viscosity (PV), (b) yield point (YP), and (c) gel strength at 10 s and 10 min after the hot rolling process

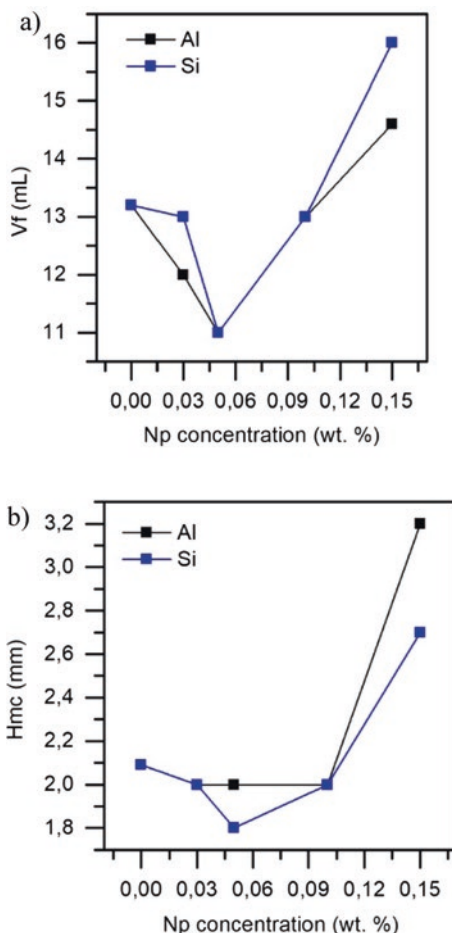


consequence of the electrochemical forces inside the fluid under dynamic conditions [22]. These electrochemical forces were improved because of the electrical charges of the nanoparticles under a pH of 10 (pH of work), and deprotonation of H⁺ of the Si–OH and Al–OH occurs, resulting in a negative charge in the ζ -potential values, -31.54 and -56.66 mV, for the Si and Al NPs, respectively. The ζ -potential value is related to the colloidal stability due to the repulsion forces between the particles; for ζ -potential lower than -30 mV, a higher stability is obtained because the repulsion forces acts between the particles [24, 37, 52]. With regard to the samples presented herein, the Si NPs presented a lower ζ -potential than the Al nanoparticles, so the repulsion forces weakly favored the aggregation, allowing a higher resistance to flow and generating high PV values.

Otherwise, the gel strength, for the concentration range of 0.03–0.05 wt.%, presented a slight increase. However, at higher concentrations, the properties improve by approximately 60% and 80% with respect to the drilling fluid sample without NPs. Additionally, the gel structure of Al NPs was better than that of the Si NPs for concentrations greater than 0.1 wt.%. The gel strength is one of the **major** rheological properties indicating the capacity to build a gel structure during static conditions allowing the solid particles and cuttings suspension [22, 53]. This means that Al NPs present better electrostatic forces under static conditions, whereas the Si NPs exhibit the highest performance while the drilling fluid is in circulation. This could be because during the circulation of the drilling fluid, there are more interactions between the polymer chains and the Si NPs than in the case of the Al NPs. The ζ -potential value is quite high for the Al NPs, so in theory, the repulsion forces govern the system; however, under static conditions, the aggregation is predominant. This suggests that the conditions of the dynamic circulation of the fluids favor the Si NP–drilling fluid interactions, whereas the static conditions favor the Al NP–drilling fluid interaction. The NPs could improve the rheological parameter of the drilling fluids through different mechanisms that depend on the continuous phase, water, of the mud system, and characteristics of the NPs, as shown in previous studies [23–25, 27, 54–56]. The Si NPs could improve the viscosity and YP of the drilling fluids and consequently the transport of the solids and cutting to the surface during the drilling operation, whereas the Al NPs are better for the suspension or solids under static conditions. The NPs dispersed in the drilling fluid have a possibility of increasing the friction between the layers, which increases the viscosity [48, 49, 54]. The NPs and polymer may be linked through certain chemical linkages, thereby increasing the PV, YP, and gel strength. These results are in good agreement with the previous findings obtained by our group.

Figure 11.4a, b show the effects of NP concentration on the filtration volume and mudcake thickness at 500 psi and 70 °C of the drilling fluid samples after the hot rolling process. The filtration volume and mudcake thickness decrease until a concentration of 0.05 wt.% and then start to increase with an increase in the NP concentration. The Si and Al NPs presented a higher reduction of 17% in the filtration volume at an optimum concentration of 0.05 wt.%. The Si NPs reduced the mudcake thickness by 18% compared with the base mud, whereas the Al NPs did not present any significant changes. However, above an NP concentration of 0.1 wt.%,

Fig. 11.4 Volume filtration (V_f) and mudcake thickness (h_{mc}) as a function of the NP concentration after the hot rolling process



a heavy filter cake thickness with a low quality was obtained, resulting in a high filtration volume. This behavior could be explained by the aggregation between the particles due to the reduction in the distance between them with the increase in the concentration. This was evident in the fact that the increments in the PV, YP, and gel strength were less at low concentrations; however, above 0.1 wt.%, the resistance to flow increases due to the aggregation. This suggests that the van der Waals and electrostatic attraction forces are predominant at high NP concentration [57]. When the Al and Si NPs are in the region of stability, that is, at ζ -potentials lower than -30 mV, we can expect a higher stability state to occupy the space between the bridging materials, and they can even act as dispersing agents [37, 58]. Some authors have reported that NPs could enhance the rheological and filtration parameters of the drilling fluids [23, 24, 26, 29, 54, 55, 59–62]. The NPs could interact with the polymer additives and strength of the viscoelastic structure [21, 23, 24, 61], while they act in the mudcake occupying the space and reducing the permeability and

porosity [24, 37, 55, 63]. Thus, the effluents from the HPHT filtration test with a concentration of 0.05 wt.%, which presented the highest filtration reduction, were selected to evaluate the possible wettability alteration, reduction in IFT, and migration fines control capacity.

11.3.3 Effluent Evaluations

Generally, the mud filtrate invaded is considered a contamination of the rock, altering the oil saturation, wettability, capillary pressure, among other properties near the wellbore [12, 18]. However, this could change with mud filtrate reduction and enhancement in the quality. This means while drilling, the mud filtrate invaded with the NPs could improve oil mobility and migration fines control because of NP retention in the porous media. Therefore, in this section, the effluents obtained in the HPHT test with an optimal NP concentration of 0.05 wt.% were selected as they showed the highest filtration reduction and improvement in the mudcake thickness to soak the sandstone core and Ottawa sands. The processes of mud filtrate invasion through the rock and wettability alteration were emulated. The results showed reduction in the IFT, improved oil mobility, and migration fines control. Figure 11.5 shows the drops of water (Fig. 11.5a–c) and oil (Fig. 11.5d–f) placed onto the rock surface, before and after mud filtrate soaking. As shown, the rock sample treated with the mud filtrate in the absence of NPs showed an average contact angle of 66.6° . This condition indicates a low oil-wet condition [64, 65]. The same behavior was observed for the rock treatment with the mud filtrate with Si NPs, 69.0° . However, the rock soaked with a mud filtrate with Al NPs presented a reduction of 37% compared with the base scenario (mud filtrate without the NPs), reaching an average contact angle of 41.4° . The presence of Al NPs favored the water-wettability, whereas the rock samples treated with the mud filtrate with the Si NPs did not

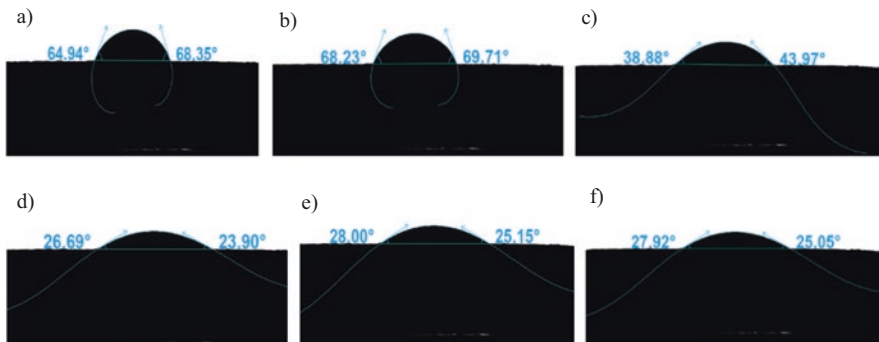
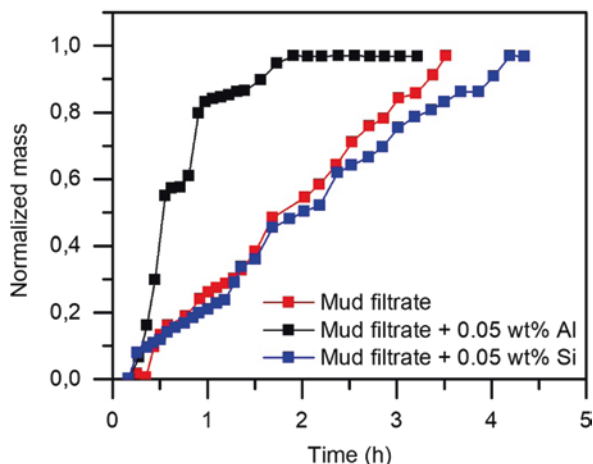


Fig. 11.5 Contact angles for the water/air/rock system treated with the mud filtrate: (a) without NPs, (b) with 0.05 wt.% Si, and (c) with 0.05 wt.% Al. Contact angles for the oil/air/rock system treated with the mud filtrate: (d) without NPs, (e) with 0.05 wt.% Si, and (f) with 0.05 wt.% Al

change the oil wettability to water. For the oil droplets, the contact angles after the mud filtrate treatment with and without the NPs did not change. Thus, the mud filtrate alters the wettability of the water but not of the oil. Subsequently, spontaneous imbibition tests were performed with the rock samples treated with the mud filtrate with and without the NPs. The difference between the former test is the available surface area in contact with the liquid. In the following test, the water could enter the rock and interact with the porous interconnected. Figure 11.6 compares the spontaneous imbibition of the rock samples treated with the mud filtrate in the absence of NPs, with 0.05 wt.% of Si and Al NPs, respectively. A fast-spontaneous imbibition was observed for the rock with the mud filtrate with Al NPs, consistent with the water-wet condition obtained in the contact angle test. This could be due to the capillary pressure, which is the main factor driving the spontaneous imbibition and is greater as the system is more water-wet, whereas the rock samples treated with the mud filtrate without the NPs presented the slowest imbibition process. These results are in good agreement with those obtained from the contact angle test. The mud filtrate that invaded the formation can improve the wettability of the rock. The NPs that have an affinity for the oil phase could be more easily adsorbed onto the surface and can extend, making a thin film between the water drop and the solid surface, as reported in literature [40, 66–68]. This means that the NPs decorate the surfaces with induced oil wettability change into water preferences [40, 69]. Regarding the IFT, the Al nanoparticles in the mud filtrate generated a reduction in the IFT measurement from 31.4 ± 0.5 mN/m to 24.1 ± 0.3 mN/m, which represents a reduction of 24% compared with the crude oil/formation brine, whereas the mud filtrate without the NPs did not represent a significant change, with IFT values of 31.9 ± 0.2 mN/m and 40 ± 0.5 mN/m, respectively. The NPs created a layer at the crude oil and brine interface, thus reducing the friction between them, improving the mobilization of the oil, and decreasing the work required to move the oil droplets [70]. The trapped oil can be recovered if the ratio between the viscous and capillary forces, expressed in literature as the capillary number $Nc = \mu V / \sigma \cos(\theta)$ [71], can

Fig. 11.6 Spontaneous imbibition curves for sandstone cores soaked with a mud filtrate in the absence and presence of Al and Si NPs with a concentration of 0.05 wt.%

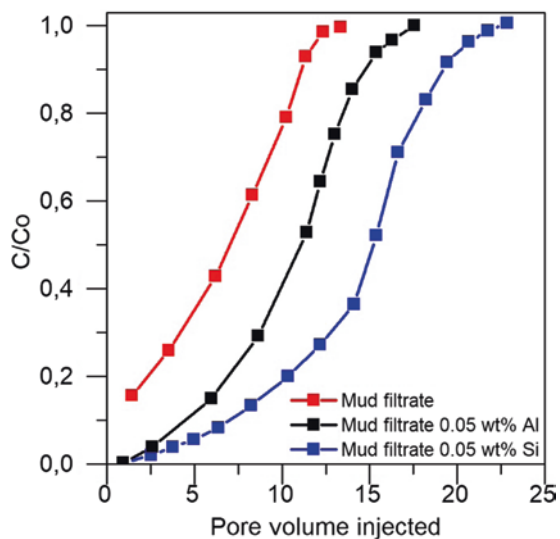


be increased when the system exhibits the least flow restriction due to the reduced interfacial and wettability. Wettability alteration and IFT reduction are two important mechanisms for enhanced oil recovery, playing a dominant role in the possible oil mobility mechanisms. The mud filtrate not only works as a conventional stimulation treatment but also helps change the wettability and reduce the IFT.

Figure 11.7 shows the breakthrough curves for the sand samples treated with the mud filtrate with and without the Al and Si NPs at 0.05 wt.%. For the mud filtrate of the base drilling fluid, the breakthrough curve shows an inherent retentive capacity to sand, which is considerably lower than that when it is impregnated with the NPs, as these provide a greater fixate capacity of the fines on the sand. Therefore, the sand sample impregnated with the mud filtrate with the Si NPs presented a greater fines retention. This could be attributed to the better affinity of the Si NPs to clay fines in attaching to the sand grains. The attractive bonds between these particles and the rock matrix are strengthened by the presence of the NPs that had been previously adsorbed onto the surface. In other words, the presence of certain NPs inhibits the fines migration by fixing them to the formation [43, 72]. These results are consistent with the report by Mora et al. [44].

Based on the obtained results, the drilling fluid with Al and Si NPs reported a filtration volume reduction and improvement in rheological properties. Additionally, the mud filtrate that invaded the formation could improve the water-wettability tendency and reduce the IFT, for the case of the mud filtrate with Al NPs, and achieve a greater retention of the fine particles that could be released from the porous media or invaded from the drilling fluid, in the case of the mud filtrate with the Si NPs. The IFT and wettability influence the capillary pressure [73]. In this sense, the reduction in the IFT and water-wet tendency enhances the mobilization of the oil and improves the oil recovery by decreasing the work required to move the oil droplets through

Fig. 11.7 Breakthrough curves for the sand samples treated with the mud filtrate in the absence and presence of 0.05 wt.% Al and Si NPs



the pore throat [70]. Therefore, the mud filtrate invaded will not represent other mechanisms of formation damage during drilling operation; otherwise, this mud filtrate could improve the properties of the rock and the formation fluids such as the conventional stimulation treatment. Finally, a dual purpose drilling fluid based on nanotechnology could be obtained through the enhancement of the drilling fluid properties and improvement of the rock properties through the enhancement of the mud filtrate quality. To corroborate the effect of these NPs under the reservoir and dynamic conditions through displacement tests, the Al NPs at 0.05 wt.% was selected owing to the filtration volume reduction, wettability alteration, IFT reduction, and fine migration control, although to a lower extent, given that the Si NPs only presented fines migration control effect and not wettability or IFT improvement.

11.3.4 Displacement Test

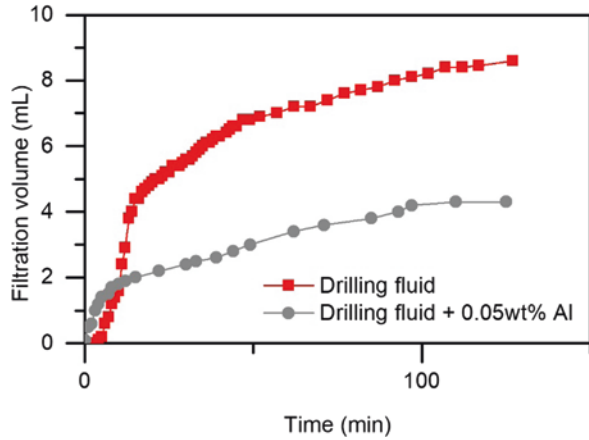
The best NP and its concentration obtained in the static test, Al 0.05 wt.%, were evaluated by conducting a dynamic filtration test through core flooding under reservoir and dynamic conditions. Table 11.2 lists the oil effective permeability for the three scenarios reported. The reduction in the oil effective permeability owing to the double purpose drilling fluid was lower than the mud unless the NPs. Finally, the return permeability of the drilling fluid without the NPs presented a good return, reaching its initial oil effective permeability. However, the drilling fluid with the NPs allowed not only the return of the permeability but also a stimulation of the permeability by 12% compared with the initial permeability value. The difference in the oil effective permeability reductions after injecting the drilling fluid with and without the NPs can be explained by the aggregation effect of the particles achieved in the presence of NPs, allowing a lower invasion of the fines particles and mud filtrate due to a less impermeable mudcake and therefore less formation damage, which can be corroborated by the reduction in the filtration volume shown in Fig 11.8.

The dynamic filtration behavior was reduced by 52% after the addition of the Al NPs to the double purpose drilling fluid, as shown in Fig. 11.8. During the first minutes, the highest filtration volume was obtained. In this scenario, the internal mudcake is in motion. However, for the drilling fluid with the NPs, the change in the

Table 11.2 Comparison of oil effective permeability reduction due to the drilling fluids with and without 0.05 wt.% Al NPs

Mud type	Drilling fluid	Drilling fluid +0.05 wt.% Al NPs
Initial permeability (mD)	393	393
Damage permeability (mD)	202	282
Permeability reduction (%)	48.6	28.2
Return permeability (mD)	390	442
Permeability reduction (%)	0.7	12.5

Fig. 11.8 Dynamic filtration curves for the drilling fluid with 0.05 wt.% Al nanoparticles



slope is faster, indicating the development of the mudcake with low permeability and porosity. For the drilling fluid without the NPs, it required more time to reach a low-permeability mudcake to allow for the reduction in the mud filtrate invasion and buildup of the external mudcake. At this time, a high filtration volume was reached. In the second stage, the external mudcake was evaluated, where a seal was developed on the wall of the wellbore. Regarding the drilling fluid with the NPs, the filtration volume tends to stop, whereas for the drilling fluid without the NPs, the external mudcake is not yet consistent, so the filtration volume increases over time. The NPs plug the pores and prevent the solid particles and mud filtrate invasion. Based on the studies carried out by our research group, the NPs improve the filter cake properties and solid packing, thus reducing the filtration volume and the growth time for a stable and low-permeability filter cake formation [37, 55, 58].

Figure 11.9 shows the relative permeability curves for the baseline, drilling fluid with and without Al NPs. Once again, the cores used in the study presented the same petrophysical properties that ensure the reproductivity of the study, meaning that it could represent the C7 formation. The Kro value at residual water saturation, endpoint, for the scenario without the NPs presented the highest reduction as a result of the highest solid particles and mud filtrate induced while circulating the drilling fluid, as reported in Fig. 11.8. However, the NP addition allowed the lowest reduction in the endpoint value. Therefore, the formation damage or the permeability reduction was the lowest. After drilling fluid without the NP circulation, the residual oil increased, and the water saturation decreased, compared with the baseline scenario. The opposite was obtained for the drilling fluid in the presence of the NPs, achieving a reduction in the Sor. This could be explained by the change in the wettability; the porous media retained water and produced crude oil. These results are consistent with the evaluation of the effluents in the static test and the reduction of the K_{rw} curves. Finally, the NPs in the drilling fluid improved the oil mobility based on the conservation of the Kro slope. The NPs could inhibit the formation damage and improve the wettability through the decoration of the porous media and reduction in the IFT, which does not occur in a conventional drilling fluid.

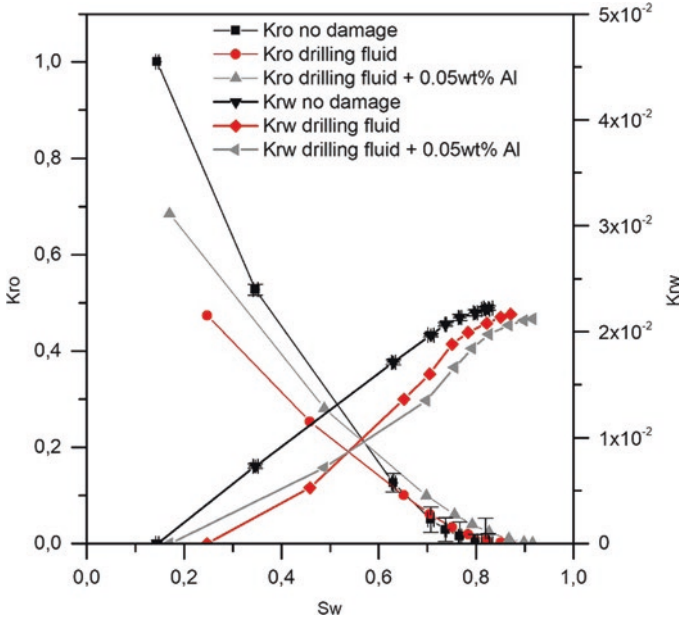


Fig. 11.9 Relative permeability curves for the scenario without damage, after the injection of the base drilling fluid and with 0.05 wt.% alumina nanoparticles (Al)

Fig. 11.10 Oil recovery factor curves for the drilling fluid with and without 0.05 wt.% Al nanoparticles

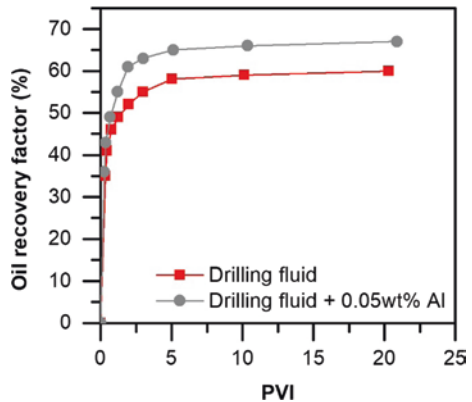


Figure 11.10 shows the oil recovery factor for the drilling fluid with and without the NPs. The drilling fluid system without the NPs showed an oil recovery of 59%. The drilling fluid with a 0.05 wt.% Al NPs provided an oil recovery of 66%, compared with the drilling fluid system without the NPs. According to this result, the NPs in the drilling fluids reduced the formation damage by the mud filtrate and solid particle invasion. Moreover, the NPs could change the wettability of the porous medium that favored the permeability return, obtaining 7% more crude oil than the conventional drilling fluid. Additionally, as mentioned before, the mud filtrate from

the double purpose drilling fluid helped reduce the IFT, indicating that the trapping oil can be recovered.

Figure 11.11 shows the behavior of K_o by varying the injection rate after the mud filtrate circulation with and without the NPs. The objective was to determine the rate at which the fines particles detach from the porous media and flow through blocking the pore spaces and reduce the permeability mudcake. The addition of the NPs to the drilling fluid and subsequent invasion of these through the mud filtrate increased

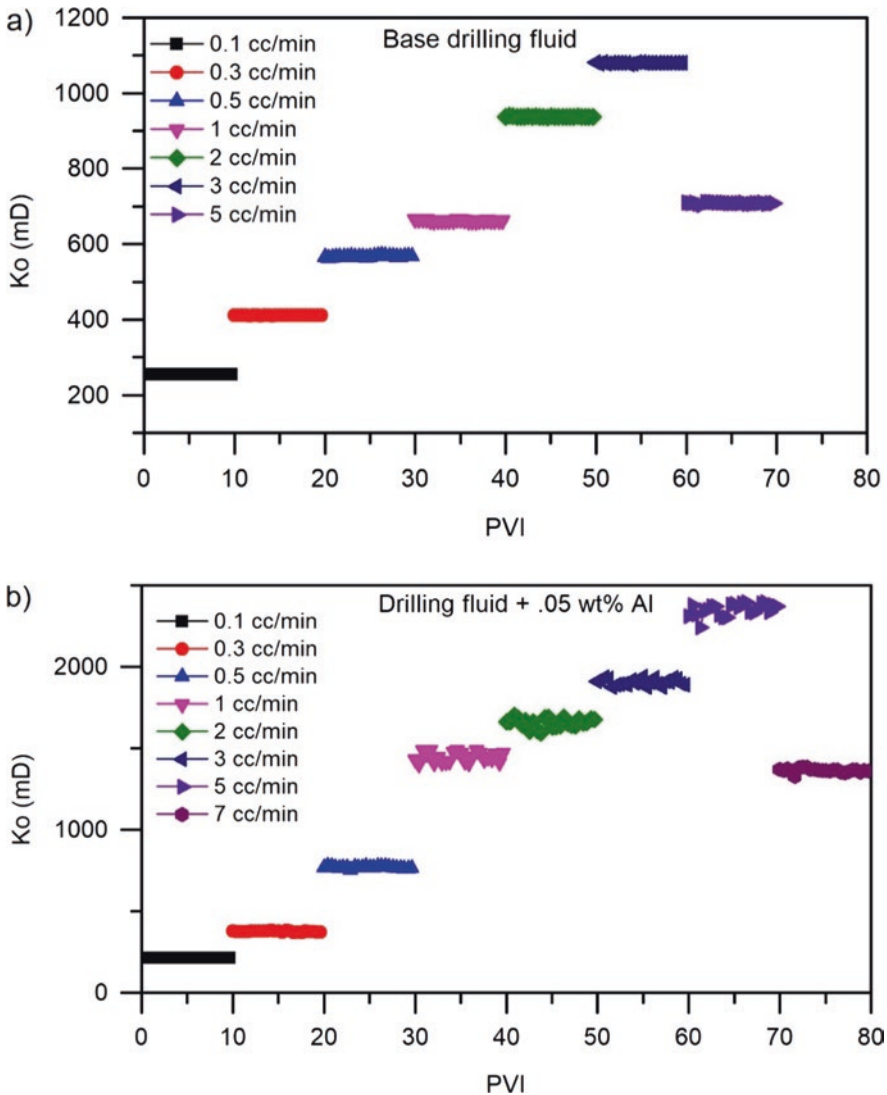


Fig. 11.11 Critical injection rate to crude oil after mud filtrate injection from (a) base drilling fluid and (b) drilling fluid with 0.05 wt.% alumina nanoparticles (Al)

the injection rate from 5 mL/min (base drilling fluid) to 7 mL/min, an increase of 25%. The NPs decorate the porous medium, and once the fines particles start migrating, they are trapped by the NPs with no possibility of migrating or plugging the throats.

11.3.5 Field Application

The main damage mechanisms of the Ocelot field have been identified, that is, drilling-induced formation damage associated with the drilling process where water-based muds are dominant. During the production life of the wells, the productivity decreases because of the migration of fines (presence of migratory clays) and wettability changes due to organic deposits (crude oil with colloidal instability). During the drilling operation of new wells, the drilling fluid allows the formation of an efficient seal that helps reduce the filtration volume and solid invasion. Additionally, the mud filtrate acts as a carrier fluid for the entry of NPs and helps improve the properties of the rock by changing the tendency of the wettability to water and controlling the fines and clay migration. Therefore, this damage mechanism is the most important during the production stage.

A pilot was carried out in July 2020 in two wells in the Ocelote field whose target formation is C7A. To evaluate the behavior in the two types of wells, the study was initially carried out in a deviated well where the risks of differential sticking are less. Subsequently, based on the results obtained, the second pilot will be run in a horizontal well in the same production unit. From the above, a more effective result is expected in the horizontal well where historically a greater invasion of mud filtration has been reported given the drilling conditions.

The validation of the results will be carried out by comparing the behavior of the pilot with a base well whose drilling will be carried out using the same drilling fluid without nanomaterials. These wells will be considered as twins and will be characterized by their similarity in terms of the structural location, target formation, mineralogy, deviation, extent of completion, types of fluids produced, and expected productivity indexes. The last parameter is directly associated with the petrophysical properties and well pressure conditions. The described comparison could help evaluate the variation in the following parameters between the twin wells in order to verify less fluid invasion, higher productivity associated with less drilling-induced formation damage, and early fine stabilization.

11.3.5.1 Invasion Diameter Calculation by Well Logging

Given the different research depths of resistivity tools and the difference between the formation water salinity and the drilling mud salinity, it is possible to define an invasion profile both in wells without the nanofluids and in wells where the technology is tested and thus compare the values in the formation of interest and quantify

the percentage of decrease. This is achieved through a statistical distribution of the resistivity curves in each of the wells.

11.3.5.2 Stabilization Time of Production Fluids

During the development of the Ocelote field, it has been found that there are wells that take longer to produce the completion fluids. These cases from a petrophysical viewpoint have been associated with poor filtration control. Given the above, the time it takes to produce the formation fluids and the volumes obtained before producing the formation fluids will be calculated, discounting for the pipeline capacities. The reservoir fluids are expected to be obtained more quickly in the pilot with the nanomaterials.

11.3.5.3 Productivity Index

The initial productivity index will be compared by normalizing per feet of open formation between the pilot wells and the comparison wells in the area. For the pilot well, a lower deviation in the real productivity index is expected due to petrophysical properties, which translates into less formation damage. Less formation damage may be associated with less invasion of the mud filtrate and restoration of the formation wettability.

11.3.5.4 Solid Production

Wellhead monitoring of the solid content produced during a month will be carried out at equal time intervals so that a low solid content can be expected in the pilot due to the stabilization of the NPs. The solids will be characterized by DRX and PSD to confirm that they correspond to fines from the reservoir.

11.4 Conclusion

Alumina and silica NPs presented enhancement in the rheological and filtration properties of a drilling fluid. The Si NPs at 0.05 wt.% presented an increase in PV of over 9% compared with the drilling fluid without the NPs. However, the Al NPs required a concentration of 0.1 wt.% to realize the same performance. The Al and Si NPs could improve the YP and gel strength of the drilling fluids, but a concentration of 0.1 wt.% was required to have significant changes. The filtration volume under HPHT conditions after the aging process was reduced by 17% when adding 0.05 wt.% of Si and Al NPs. The Si NPs reduced the mudcake thickness by 18%.

The AI NPs exhibited the highest performance in terms of the contact angle reduction, 37%, IFT reduction 44%, and fine migration control, 66%. This indicates that the NPs invaded through the mud filtrate could generate a water-wettability tendency and retain the fines during the production time. Thus, the AI NPs were selected for evaluation in displacement tests, not only owing to better filtration reduction but also in terms of improving the oil mobility.

The AI NPs at 0.05 wt% in the drilling fluid reduce the filtration volume under dynamic conditions by 52.1%, and the decrease in the oil effective permeability due to the double purpose drilling fluid was lower than that of the mud without the NPs by 20.2%. The NPs inhibited the formation damage owing to the reduction in the invasion of filtrate and solid particles. The system allowed a high water retention by increasing the saturation window, thus improving the mobility of the oil. These characteristics provided an additional recovery of 10% crude compared with the baseline scenario.

The AI NPs serve two objectives in the drilling fluid. After the drilling fluid circulation, an increase in the critical injection rate of 66% was observed, indicating a greater stability of the fines in the porous media. Thus, the treatment shows a potential not only to reduce the damage by the drilling fluids but also as an agent for fine migration.

The results (field application) are in the process of execution, starting from the selection of drilling fluids and wells that meet the requirements, wells with percentage of damage induced during drilling, fines migration, deposition of organics, and subsequent changes in the wettability during the production life. Additionally, we expect that the results will help compare the invasion diameter, well stabilization time, productivity index, and solid production in the two wells called twin wells, one of which will be drilled without the NPs and the other using the mud with NPs based on its formulation.

Acknowledgments The authors want to thank HOCOL S.A for granting permission to present and publish this paper and Engineers Oscar Medina and Johanna Roldán for their help in the experimental tests. We would also like to recognize the Universidad Nacional de Colombia and Colciencias for logistical and financing assistance in the doctoral studies of Johanna Vargas Clavijo through the announcement of 785/2018.

References

1. B. Peng, S. Peng, B. Long, Y. Miao, W.Y. Guo, Properties of high-temperature-resistant drilling fluids incorporating acrylamide/(acrylic acid)/(2-acrylamido-2-methyl-1-propane sulfonic acid) terpolymer and aluminum citrate as filtration control agents. *J. Vinyl Addit. Technol.* **16**, 84–89 (2010)
2. M. Aston, P. Mihalik, J. Tunbridge, S. Clarke, Towards zero fluid loss oil based muds, in *SPE Annual Technical Conference and Exhibition* (2002)
3. D. Jiao, M.M. Sharma, Dynamic filtration of invert-emulsion muds. *SPE Drill. Complet.* **8**, 165–169 (1993)

4. S. Gharat, J. Azar, D. Teeters, Effect of incompatibilities caused by fluids filtrates on formation properties, in *SPE Formation Damage Control Symposium* (1994)
5. D.B. Bennion, R.F. Bietz, F.B. Thomas, M.P. Cimolai, Reductions in the productivity of oil and low permeability gas reservoirs due to aqueous phase trapping. *J. Can. Pet. Technol.* **33**, 45–54 (1994)
6. D. Jia, J. Buckley, and N. Morrow, Alteration of wettability by drilling mud filtrates, in *SCA Symposium*, Norway, September (1994)
7. G. Phelps, G. Stewart, J. Peden, The effect of filtrate invasion and formation wettability on repeat formation tester measurements, in *European Petroleum Conference* (1984)
8. A. Wojtanowicz, Z. Krilov, J. Langlinais, Experimental determination of formation damage pore blocking mechanisms. *J. Energy Resour. Technol.* **110**, 34–42 (1988)
9. R. Caenn, H. Darley, G. Gray, Chapter 10—Completion, reservoir drilling, workover, and packer fluids, in *Composition and Properties of Drilling and Completion Fluids*, 6th edn., (Gulf Professional Publishing, Boston, 2011), pp. 477–533
10. J. Argillier, A. Audibert, D. Longeron, Performance evaluation and formation damage potential of new water-based drilling formulas. *SPE Drill. Complet.* **14**, 266–273 (1999)
11. R. Caenn, H.C.H. Darley, G.R. Gray, Chapter 7 – The filtration properties of drilling fluids11a glossary of notation used in this chapter will be found immediately following this chapter's text, in *Composition and Properties of Drilling and Completion Fluids*, ed. by R. Caenn, H. C. H. Darley, G. R. Gray, 7th edn., (Gulf Professional Publishing, Boston, 2017), pp. 245–283
12. R. Caenn, H.C.H. Darley, G.R. Gray, Chapter 10 – Drilling problems related to drilling fluids, in *Composition and Properties of Drilling and Completion Fluids*, ed. by R. Caenn, H. C. H. Darley, G. R. Gray, 7th edn., (Gulf Professional Publishing, Boston, 2017), pp. 367–460
13. A. Suri, M.M. Sharma, Strategies for sizing particles in drilling and completion fluids. *SPE J.* **9**, 13–23 (2004)
14. M. Dick, T. Heinz, C. Svoboda, M. Aston, Optimizing the selection of bridging particles for reservoir drilling fluids, in *SPE International Symposium on Formation Damage Control* (2000)
15. W. He, M. P. Stephens, Bridging particle size distribution in drilling fluid and formation damage, in *SPE European Formation Damage Conference* (2011)
16. S. Vickers, M. Cowie, T. Jones, A.J. Twynam, A new methodology that surpasses current bridging theories to efficiently seal a varied pore throat distribution as found in natural reservoir formations. *Wiernictwo, Nafta, Gaz* **23**, 501–515 (2006)
17. H.C. Darley, G.R. Gray, *Composition and Properties of Drilling and Completion Fluids* (Gulf Professional Publishing, Boston, 1988)
18. F. Civan, Chapter 18—Drilling mud filtrate and solids invasion and mudcake formation, in *Reservoir Formation Damage*, (Gulf Professional Publishing, Burlington, 2007)
19. M. Al-Yasiri, D. Wen, Gr-Al₂O₃ nanoparticles based multi-functional drilling fluid. *Ind. Eng. Chem. Res.* **58**, 23 (2019)
20. S. M. Javeri, Z. M. W. Haindade, C. B. Jere, Mitigating loss circulation and differential sticking problems using silicon nanoparticles, in *SPE/IADC Middle East Drilling Technology Conference and Exhibition* (2011)
21. A. Salih, T. Elshehabi, H. Bilgesu, Impact of nanomaterials on the rheological and filtration properties of water-based drilling fluids, in *SPE Eastern Regional Meeting* (2016)
22. A.E. Bayat, P.J. Moghanloo, A. Piroozian, R. Rafati, Experimental investigation of rheological and filtration properties of water-based drilling fluids in presence of various nanoparticles. *Colloids Surf. A Physicochem. Eng. Asp.* **555**, 256–263 (2018)
23. S.R. Smith, R. Rafati, A. Sharifi Haddad, A. Cooper, H. Hamidi, Application of aluminium oxide nanoparticles to enhance rheological and filtration properties of water based muds at HPHT conditions. *Colloids Surf. A Physicochem. Eng. Asp.* **537**, 361–371 (2018)

24. M.M. Barry, Y. Jung, J.-K. Lee, T.X. Phuoc, M.K. Chyu, Fluid filtration and rheological properties of nanoparticle additive and intercalated clay hybrid bentonite drilling fluids. *J. Pet. Sci. Eng.* **127**, 338–346 (2015)
25. Y. Jung, Y.-H. Son, J.-K. Lee, T.X. Phuoc, Y. Soong, M.K. Chyu, Rheological behavior of clay–nanoparticle hybrid-added bentonite suspensions: Specific role of hybrid additives on the gelation of clay-based fluids. *ACS Appl. Mater. Interfaces* **3**, 3515–3522 (2011)
26. M.-C. Li, Q. Wu, K. Song, C.F. De Hoop, S. Lee, Y. Qing, et al., Cellulose nanocrystals and polyanionic cellulose as additives in bentonite water-based drilling fluids: Rheological modeling and filtration mechanisms. *Ind. Eng. Chem. Res.* **55**, 133–143 (2015)
27. M.-C. Li, Q. Wu, K. Song, Y. Qing, Y. Wu, Cellulose nanoparticles as modifiers for rheology and fluid loss in bentonite water-based fluids. *ACS Appl. Mater. Interfaces* **7**, 5006–5016 (2015)
28. L. Liu, X. Pu, K. Rong, Y. Yang, Comb-shaped copolymer as filtrate loss reducer for water-based drilling fluid. *J. Appl. Polym. Sci.* **135**, 45989 (2018)
29. J.K.M. William, S. Ponmani, R. Samuel, R. Nagarajan, J.S. Sangwai, Effect of CuO and ZnO nanofluids in xanthan gum on thermal, electrical and high pressure rheology of water-based drilling fluids. *J. Pet. Sci. Eng.* **117**, 15–27 (2014)
30. S.S. Hassani, A. Amrollahi, A. Rashidi, M. Soleymani, S. Rayatdoost, The effect of nanoparticles on the heat transfer properties of drilling fluids. *J. Pet. Sci. Eng.* **146**, 183–190 (2016)
31. M. Sedaghatzadeh, A. Khodadadi, An improvement in thermal and rheological properties of water-based drilling fluids using multiwall carbon nanotube (MWCNT). *Iran. J. Oil Gas Sci. Technol.* **1**, 55–65 (2012)
32. J. Cai, M.E. Chenevert, M.M. Sharma, J.E. Friedheim, Decreasing water invasion into Atoka shale using nonmodified silica nanoparticles. *SPE Drill. Complet.* **27**, 103–112 (2012)
33. P.J. Boul, B. Reddy, J. Zhang, C. Thaemlitz, Functionalized nanosilicas as shale inhibitors in water-based drilling fluids. *SPE Drill. Complet.* **32**, 121–130 (2017)
34. Y. Kang, J. She, H. Zhang, L. You, M. Song, Strengthening shale wellbore with silica nanoparticles drilling fluid. *Petroleum* **2**, 189–195 (2016)
35. M. Amanullah, An environment friendly and economically attractive thermal degradation inhibitor for bentonite mud, in *SPE Europec/EAGE Annual Conference and Exhibition* (2006)
36. D. Longeron, J. Argillier, A. Audibert, An integrated experimental approach for evaluating formation damage due to drilling and completion fluids, in *SPE European Formation Damage Conference* (1995)
37. J.V. Clavijo, L.J. Roldán, L. Valencia, S.H. Lopera, R.D. Zabala, J.C. Cárdenas, et al., Influence of size and surface acidity of silica nanoparticles on inhibition of the formation damage by bentonite-free water-based drilling fluids. Part I: Nanofluid design based on fluid-nanoparticle interaction. *Adv. Nat. Sci. Nanosci. Nanotechnol.* **10**, 045020 (2019)
38. R. API, *13B-1: Recommended Practice for Field Testing Water-Based Drilling Fluids, and ISO 10414-1* (American Petroleum Institute, Washington, DC, 2003)
39. M. Franco-Aguirre, R.D. Zabala, S.H. Lopera, C.A. Franco, F.B. Cortés, Interaction of anionic surfactant-nanoparticles for gas-wettability alteration of sandstone in tight gas-condensate reservoirs. *J. Nat. Gas Sci. Eng.* **51**, 53–64 (2018)
40. J. Giraldo, P. Benjumea, S. Lopera, F.B. Cortés, M.A. Ruiz, Wettability alteration of sandstone cores by alumina-based nanofluids. *Energy Fuel* **27**, 3659–3665 (2013)
41. X. Liu, F. Civan, Formation damage and skin factor due to filter cake formation and fines migration in the near-wellbore region," in *SPE Formation Damage Control Symposium* (1994)
42. C. Céspedes Chávarro, *Desarrollo de un nanofluido para la estabilización de finos de la formación barco del campo Cupiagua* (Universidad Nacional de Colombia-Sede Medellín, Medellín)
43. C. Franco Ariza, F. Cortés, D. Arias-Madrid, E. Taborda, N. Ospina, R. Zabala, et al., "Inhibition of the formation damage due to fine migration on low-permeability reservoirs of sandstone using silica-based nanofluids: from laboratory to a successful field trial.," 2018, p. 231 New York : Nova Science Publishers

44. C.M. Mera, C.A.F. Ariza, F.B. Cortés, Uso de nanopartículas de sílice para la estabilización de finos en lechos empacados de arena Ottawa. *Informador Técnico* **77**, 27–34 (2013)
45. C.H. van der Zwaag, Benchmarking the formation damage of drilling fluids, in *SPE International Symposium and Exhibition on Formation Damage Control* (2004)
46. L.F. Isernia, FTIR study of the relation, between extra-framework aluminum species and the adsorbed molecular water, and its effect on the acidity in ZSM-5 steamed zeolite. *Mater. Res.* **16**, 792–802 (2013)
47. B. Gohari, N. Abu-Zahra, Polyethersulfone membranes prepared with 3-aminopropyltriethoxysilane modified alumina nanoparticles for Cu (II) removal from water. *ACS Omega* **3**, 10154–10162 (2018)
48. J.R. Kennedy, K.E. Kent, J.R. Brown, Rheology of dispersions of xanthan gum, locust bean gum and mixed biopolymer gel with silicon dioxide nanoparticles. *Mater. Sci. Eng. C* **48**, 347–353 (2015)
49. L.J. Giraldo, M.A. Giraldo, S. Llanos, G. Maya, R.D. Zabala, N.N. Nassar, et al., The effects of SiO₂ nanoparticles on the thermal stability and rheological behavior of hydrolyzed polyacrylamide based polymeric solutions. *J. Pet. Sci. Eng.* **159**, 841–852 (2017)
50. J.J. Adams, Asphaltene adsorption, a literature review. *Energy Fuel* **28**, 2831–2856 (2014)
51. N.K. Maurya, A. Mandal, Studies on behavior of suspension of silica nanoparticle in aqueous polyacrylamide solution for application in enhanced oil recovery. *Pet. Sci. Technol.* **34**, 429–436 (2016)
52. A.L. Lorenzen, T.S. Rossi, I.C. Riegel-Vidotti, M. Vidotti, Influence of cationic and anionic micelles in the (sono) chemical synthesis of stable Ni (OH)₂ nanoparticles: “In situ” zeta-potential measurements and electrochemical properties. *Appl. Surf. Sci.* **455**, 357–366 (2018)
53. R. Caenn, H.C.H. Darley, G.R. Gray, Chapter 6 – The rheology of drilling fluids, in *Composition and Properties of Drilling and Completion Fluids*, ed. by R. Caenn, H. C. H. Darley, G. R. Gray, 7th edn., (Gulf Professional Publishing, Boston, 2017), pp. 151–244
54. A.R. Ismail, N.M. Rashid, M.Z. Jaafar, W.R.W. Sulaiman, N.A. Buang, Effect of nanomaterial on the rheology of drilling fluids. *J. Appl. Sci.* **14**, 1192 (2014)
55. J. Vargas, L. J. Roldán, S. H. Lopera, J. C. Cardenas, R. D. Zabala, C. A. Franco, et al., Effect of silica nanoparticles on thermal stability in bentonite free water-based drilling fluids to improve its rheological and filtration properties after aging process, in *Offshore Technology Conference Brasil* (2019)
56. Z. Vryzas, L. Nalbandian, V.T. Zaspalis, V.C. Kelessidis, How different nanoparticles affect the rheological properties of aqueous Wyoming sodium bentonite suspensions. *J. Pet. Sci. Eng.* **173**, 941–954 (2019)
57. J. Jiang, G. Oberdörster, P. Biswas, Characterization of size, surface charge, and agglomeration state of nanoparticle dispersions for toxicological studies. *J. Nanopart. Res.* **11**, 77–89 (2009)
58. S. Bentacur, F.B. Cortés, G.A.A. Espinosa, Mejoramiento de los fluidos de perforación usando nanopartículas funcionalizadas: Reducción de las pérdidas de filtrado y del espesor de la retorta. *Boletín de Ciencias de la Tierra*, 5–14 (2014)
59. M. Zakaria, M.M. Husein, G. Harland, Novel nanoparticle-based drilling fluid with improved characteristics, in *SPE International Oilfield Nanotechnology Conference and Exhibition* (2012)
60. L. Whatley, R. Barati, Z. Kessler, J.-S. Tsau, Water-based drill-in fluid optimization using polyelectrolyte complex nanoparticles as a fluid loss additive, in *SPE International Conference on Oilfield Chemistry* (2019)
61. Z. Vryzas, V.C. Kelessidis, M.B.J. Bowman, L. Nalbantian, V. Zaspalis, O. Mahmoud, et al., Smart magnetic drilling fluid with in-situ rheological controllability using Fe₃O₄ nanoparticles, in *SPE Middle East Oil and Gas Show and Conference, MEOS, Proceedings* (2017), pp. 2558–2569
62. J.T. Srivatsa, M.B. Ziaja, An experimental investigation on use of nanoparticles as fluid loss additives in a surfactant – Polymer based drilling fluid, in *Society of Petroleum Engineers – International petroleum technology conference 2012, IPTC 2012* (2012), pp. 2436–2454

63. N.C. Mahajan, B.M. Barron, Bridging particle size distribution: A key factor in the designing of non-damaging completion fluids, in *SPE Formation Damage Symposium* (1980)
64. W. Anderson, Wettability literature survey-part 2: Wettability measurement. *J. Pet. Technol.* **38**, 1246–1262 (1986)
65. A. Cassie, S. Baxter, Wettability of porous surfaces. *Trans. Faraday Soc.* **40**, 546–551 (1944)
66. K. Kondiparty, A.D. Nikolov, D. Wasan, K.-L. Liu, Dynamic spreading of nanofluids on solids. Part I: Experimental. *Langmuir* **28**, 14618–14623 (2012)
67. S. Al-Anssari, S. Wang, A. Barifcani, M. Lebedev, S. Iglauer, Effect of temperature and SiO₂ nanoparticle size on wettability alteration of oil-wet calcite. *Fuel* **206**, 34–42 (2017)
68. H. Jang, W. Lee, J. Lee, Nanoparticle dispersion with surface-modified silica nanoparticles and its effect on the wettability alteration of carbonate rocks. *Colloids Surf. A Physicochem. Eng. Asp.* **554**, 261–271 (2018)
69. C. Franco, E. Patiño, P. Benjumea, M.A. Ruiz, F.B. Cortés, Kinetic and thermodynamic equilibrium of asphaltene sorption onto nanoparticles of nickel oxide supported on nanoparticulated alumina. *Fuel* **105**, 408–414 (2013)
70. A. Roustaei, S. Saffarzadeh, M. Mohammadi, An evaluation of modified silica nanoparticles' efficiency in enhancing oil recovery of light and intermediate oil reservoirs. *Egypt. J. Pet.* **22**, 427–433 (2013)
71. L.J. Giraldo, J. Gallego, J.P. Villegas, C.A. Franco, F.B. Cortés, Enhanced waterflooding with NiO/SiO₂ 0-D Janus nanoparticles at low concentration. *J. Pet. Sci. Eng.* **174**, 40–48 (2019)
72. N.C. Ogolo, O.A. Olafuyi, M. Onyekonwu, Effect of nanoparticles on migrating fines in formations, in *SPE International Oilfield Nanotechnology Conference and Exhibition* (2012)
73. W.G. Anderson, Wettability literature survey-part 4: Effects of wettability on capillary pressure. *J. Pet. Technol.* **39**, 1283–1300 (1987)